

## Spin Polarization in CrO<sub>2</sub>: Competition between Quasiparticle and Local-Moment Behavior

Michel van Veenendaal and A. J. Fedro

*Dept. of Physics, Northern Illinois University, De Kalb, Illinois 60115  
Argonne National Laboratory, 9700 South Cass Avenue, Argonne, Illinois 60439*

(Dated: December 5, 2003)

We show that inclusion of the competition between quasiparticle and local-moment behavior in CrO<sub>2</sub> is necessary to obtain good agreement between the calculated and experimentally observed spin polarization. By going beyond a single Slater determinant description, we find a spin polarization of close to 100% near the Fermi level reflecting quasi-particle behavior. At energies higher than 0.1-0.2 eV above the Fermi level, the local moment character dominates and the spin polarization is reduced to approximately 50%.

PACS numbers: PACS numbers: 71.10.-w,75.10.Lp,75.50.Ss

The ever-increasing demands on electronics require a further shrinking of the feature sizes that has pushed the silicon technology to its limits. A promising candidate for a new device technology is spin electronics or spintronics, where the spin adds a degree of freedom to the conventional charge-based semiconductor technology[1]. An important concept in spintronics is the degree of spin polarization. As pointed out by Mazin[2], the definition of spin polarization depends strongly on the experiments under consideration. However, the most natural definition is  $(\rho_{\uparrow} - \rho_{\downarrow})/(\rho_{\uparrow} + \rho_{\downarrow})$ ; i.e. the difference between the spin-up and spin-down density of states normalized to the total density of states. This spin polarization is measured in spin-resolved (inverse) photoemission. Other experiments, such as transport measurements or Andreev reflection, probe a different degree of spin polarization[2]. In order for the spin current to pass through many different materials and interfaces while retaining a high signal-to-noise ratio, a high degree of spin polarization is essential. For example, for compatibility with conventional semiconductors, a spin polarization of close to 100% is necessary if the conductivity of the ferromagnet is to be much larger than that of the semiconductor[3]. Obviously, this makes a fundamental theoretical understanding of this concept essential.

A compound where a spin polarization close to 100% is expected[4] is CrO<sub>2</sub>, well known from its use in magnetic recording tapes. The electronic structure of CrO<sub>2</sub> has been studied extensively using theoretical models that incorporate the effects of electron-electron interactions in various ways[4–7]. In CrO<sub>2</sub>, Chromium is formally in a tetravalent (4+) state and has two electrons in the  $t_{2g}$  orbitals. CrO<sub>2</sub> is also metallic, although close to a metal-insulator transition [6]. In the rutile structure, the CrO<sub>6</sub> octahedra are essentially arranged in ribbons, splitting the  $t_{2g}$  states into two distinct bands. The band consisting of  $xy$  orbitals is full. The other two  $t_{2g}$  orbitals form a half-filled band crossing the Fermi level. The density of states in CrO<sub>2</sub> has been calculated using various methods: LDA[4, 5], LDA+ $U$ [6], and LDA plus dynamical mean field[7]. The results of these calculations are shown in the lower half of Fig. 1. The major differ-

ences focus on a number of points. First, the position of the  $xy$  band gives rise to the sharp peak below the Fermi level around 0.5 eV in the LDA calculation[4, 5]. In the LDA+ $U$  calculation[6], these states are pushed to lower energy as a result of electron-electron interactions. The other significant difference is the position of the spin-down band. In a conventional LDA calculation, the spin-down band begins at 0.5 eV above the Fermi level. Inclusion of electron-electron interactions in a Hartree-Fock fashion in LDA+ $U$  pushes the spin-down band approximately 1.5 eV higher in energy, see Fig. 1(a). In LDA plus dynamical mean field (which uses the LDA+ $U$  calculation as a starting point)[7], Coulomb interactions are treated in a more advanced way by inclusion of dynamical many-body effects. This leads to the appearance of incoherent spectral weight (Hubbard-like bands) in the spin-up density of states, see Fig. 1(b). Note that these calculations include only  $t_{2g}$  orbitals. These incoherent states “compress” the quasiparticle bands, and in fact, the spin-up density of states near the Fermi level resembles more closely the LDA calculation than the LDA+ $U$  calculation. Also the spin-down density of states is closer to the Fermi level with respect to LDA+ $U$  as a result of a Hartree shift[7]. In addition, the dynamical mean-field calculation causes a broadening of the spectral features.

Of interest to our discussion is the spin polarization seen in the upper half of Fig. 1. In fact, the qualitative behavior is very similar for the different calculations described above. Since the ground state is fully polarized only spin-up electrons can be removed and the spin polarization is 100% below the Fermi level. Above the Fermi level, the spin polarization is 100% up to the onset of the spin-down density of states, when the spin polarization becomes negative. The energy where this sign change occurs depends on the different incorporations of the many-body effects.

On the electron-removal side, these calculations should be compared with spin-resolved photoemission. Although no high-resolution experiments close to the Fermi level are available, at 2 eV below the Fermi level the spin polarization is still close to 100% [8]. This confirms our expectation of a fully polarized ground state.

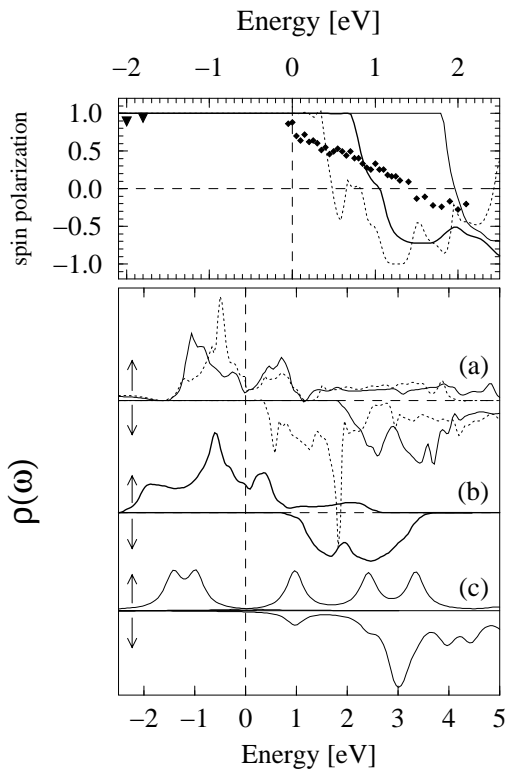


FIG. 1: The lower half shows different calculations of the spin-polarized  $\text{CrO}_2$  density of states: LDA[2] (dotted line in (a)), LDA+ $U$ [6] (solid line in (a)), LDA plus dynamical mean field[7] (thick solid line in (b)), and a configuration interaction calculation (c). The upper half shows the corresponding spin polarizations for the LDA-based densities of states. For comparison the spin polarization obtained with spin-resolved photoemission[8] (triangles) and spin-resolved oxygen 1s x-ray absorption[9] (diamonds) are shown.

The spin polarization above the Fermi level has recently been determined using spin-resolved oxygen 1s x-ray absorption[9]. By using the spin conservation of the oxygen  $KLL$  Auger decay channel, the spin polarized O  $2p$  projected density of states can be obtained. The oxygen  $2p$  spin polarization reflects well the chromium  $3d$  spin polarization within the first 2 eV above the Fermi level. The measured spin polarization looks very different from the LDA-based calculations. Close to the Fermi level, the measured spin polarization is almost 100%. However, it then slowly decreases and changes sign around 1.5 eV. In fact, apart from the high spin polarization close to the Fermi level, this behavior resembles more a local-moment behavior. For comparison, we have performed a configuration interaction calculation for a  $\text{CrO}_6$  cluster (including configurations  $3d^{n+m}\underline{L}^m$  with  $n = 2, 1, 3$  for ground state and electron-removal and addition final states, respectively;  $m = 0, \dots, 3$ , where  $\underline{L}$  stands for a hole on the oxygens surrounding the chromium), see Fig. 1(c). The calculation includes the full  $dd$  multiplet interaction and  $3d$  spin-orbit coupling[10]. For the calculation, we use a

charge-transfer energy of 4 eV and a local Coulomb interaction expressed in Racah parameters  $A = 4$ ,  $B = 0.11$  and  $C = 0.43$  eV [10]. Note that the effective gap obtained for these parameters,  $U_{\text{eff}} = A_{\text{eff}} + B = 2$  eV is significantly smaller than the bare Coulomb interaction of 4 eV as a result of the strong mixing of the Cr  $3d$  states and the surrounding oxygens. Obviously, this calculation offers a poor description of the electronic structure of  $\text{CrO}_2$  predicting it to be an insulator. However, some important points can be noted. Again, below the Fermi level, the spin polarization is 100%. For addition of a spin-down  $t_{2g}$  electron, the probability of reaching the doublet state ( $S = \frac{1}{2}$ ) is three times that of the the quartet state ( $S = 3/2$ ) [10]. The spin polarization within a configuration interaction approach is therefore  $(1 - \frac{1}{3}) / (1 + \frac{1}{3}) = 50\%$ , which is much closer to the experimentally observed value. *This leads to the important conclusion that the electronic structure in  $\text{CrO}_2$  within 1 eV above the Fermi level has a dualistic character[9]: quasiparticle-like behavior with a spin polarization close to 100% close to the Fermi level and local-moment character with a spin polarization close to 50% at higher energies above the Fermi level.* In this Letter, we show that a better description of the spin polarization can be obtained by taking into account the competition between quasiparticle and local moment character.

In  $\text{CrO}_2$ , the  $t_{2g}$  states split into an  $xy$  band which is full and two nearly degenerate states  $\tau_a = yz \pm zx$ [6] with  $a = 0, 1$  that form a half-filled band that crosses the Fermi level. Within an ionic picture, the local moments are given by  $|d_{i,xy\uparrow}d_{i\tau_a\uparrow}(^3E)\rangle$ , where  $d_{im\sigma}$  corresponds to an electron in a  $3d$  orbital with orbital index  $m$  and spin component  $\sigma$  on site  $i$ . The symmetry  $\Gamma_0 = ^3E$  is given for the local  $D_{4h}$  group[10]. Although this state minimizes the local Hamiltonian  $H_0 + H_U$  consisting of on-site energies and the full-multiplet Coulomb interaction, restriction to purely local states obviously does not minimize the kinetic energy,

$$T = \sum_{im,jm'\sigma} t(im,jm')d_{jm'\sigma}^\dagger d_{im\sigma} + \text{H.c.} \quad (1)$$

In order to find local states that provide a better balance between the kinetic energy and the on-site Coulomb interaction, let us consider the effect of the kinetic energy on a particular site. We consider the coupling of the local moment to its surroundings. For the ground state, we can restrict ourselves to the  $d_{\tau_a\uparrow}$  states, since LDA shows that all other  $3d$  orbitals are either full or empty. For a particular site, coupling to a bath of states can be expressed as a local field

$$T_{\text{local}} = \sum_a t_{\text{eff}} \left\{ d_\mu^\dagger d_{\tau_a\uparrow} + d_{\tau_a\uparrow}^\dagger d_\mu \right\}, \quad (2)$$

where site indices have been omitted and  $d_\mu^\dagger$  creates an electron in the bath with an energy equal to the chemical potential. In the case that the coupling is entirely determined by the coupling strength  $t_{\text{eff}}$ ,  $T_{\text{local}}$  corresponds

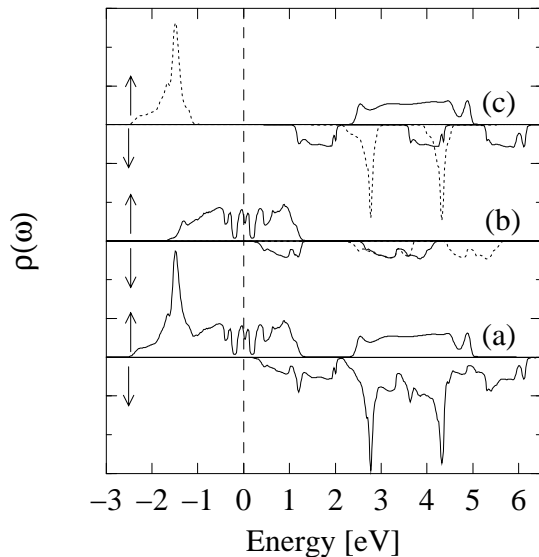


FIG. 2: The density of states for  $\text{CrO}_2$ : (a) the total density of states; (b) the  $\tau_a$ -projected density of states (solid and dotted line); (c) the  $e_g$  (solid line) and the  $xy$  (dotted line) projected density of states.

to a scalar field which induces particles on and off the site. This leads to an effective coupling between states with different numbers of particles at a particular site. The effective coupling parameter will be determined from minimization of the free energy. For the ground state, the effective local states are

$$\begin{aligned} |(xy \uparrow, \tau_a \uparrow)^{\text{eff}}\rangle &= \cos \theta |d_{xy\uparrow} d_{\tau_a\uparrow}(^3E)\rangle + \\ &(-1)^a \frac{\sin \theta}{\sqrt{2}} \{ |d_{xy\uparrow}(^2B_{2g})\rangle + (-1)^a |d_{xy\uparrow} d_{\tau_0\uparrow} d_{\tau_1\uparrow}(^4B_1)\rangle \}, \end{aligned} \quad (3)$$

where  $a = 0, 1$ ; electrons and holes in the bath have been omitted from the notation. The ionic states  $|d^n(\Gamma)\rangle$  have now been replaced by effective local states  $|\alpha\rangle$  which diagonalize  $H_0 + H_U + T_{\text{local}}$ . In addition to the two effective local-moment states  $|(xy \uparrow, \tau_a \uparrow)^{\text{eff}}\rangle$ , there are also their electron-removal ( $|(xy \uparrow)^{\text{eff}}\rangle$ ) and electron-addition ( $|(xy \uparrow, \tau_0 \uparrow, \tau_1 \uparrow)^{\text{eff}}\rangle$ ) counterparts.

The dispersion of these effective local states can be obtained from the Green's function

$$G_{im\sigma}^{jm'\sigma}(t) = -i \langle g | \{ d_{jm'\sigma}(t), d_{im\sigma}^\dagger(0) \} | g \rangle, \quad (4)$$

where  $|g\rangle$  is the ground state consisting of effective local states  $|\tau_a\rangle$ . The Fourier transform of the Green's function is split into an electron-removal and an electron-addition part

$$\begin{aligned} G_{i\alpha'}^{j\alpha'}(\omega) &= \sum_{aa'mm'\sigma\sigma'} \quad (5) \\ &\left\{ \langle j\tau_{a'} | d_{jm'\sigma}^\dagger | j\alpha' \rangle \langle j\alpha' | \frac{1}{z-H} | i\alpha \rangle \langle i\alpha | d_{im\sigma} | i\tau_a \rangle \right. \\ &\left. + \langle j\tau_{a'} | d_{jm'\sigma} | j\alpha' \rangle \langle j\alpha' | \frac{1}{z+H} | i\alpha \rangle \langle i\alpha | d_{im\sigma}^\dagger | i\tau_a \rangle \right\}, \end{aligned}$$

where  $z = \omega + i0^+$ . The Green's function describes the dispersion of an excited local state in a background of  $|i\tau_a\rangle$  states, where  $|i\tau_a\rangle$  is shorthand for  $|i(xy, \tau_a)^{\text{eff}}\rangle$ . Note that in the Green's function, we have to include all possible configurations  $|\alpha\rangle$  that can be reached from the ground state. When we restrict ourselves to the coherent motion of the excited local states, we can solve the total Green's function by going to  $\mathbf{k}$  space:

$$G_{\mathbf{k}m\sigma} = \sum_{\alpha\alpha'} G_{\mathbf{k}m\sigma,\alpha}^{\alpha'} = \frac{1}{(G_{m\sigma}^0)^{-1} - \varepsilon_{\mathbf{k}m\sigma}}, \quad (6)$$

where the band energies are taken from the spin-polarized independent-particle density of states[5]. We have assumed here that cross terms between  $3d$  states of different symmetry, i.e.  $m = xy, \tau, e_g$ , and between spin-up and spin-down bands are small and will be neglected. The local Green's function is given by

$$G_{m\sigma}^0 = \frac{1}{2} \sum_{\alpha} \frac{|\langle \alpha | d_{m\sigma}^\dagger | \tau_a \rangle|^2}{z - E(\alpha)}, \quad (7)$$

where the local energies are given by  $E(\alpha) = \langle \alpha | H_0 + H_U | \alpha \rangle$ .

Quasiparticle behavior is found only for the  $\tau_a \uparrow$  states ( $\tau_{0,1} = yz \pm zx$ ). The  $\tau_a \uparrow$  states form a Hubbard-like system, where the orbital index  $a = 0, 1$  replaces the spin  $\sigma = \uparrow, \downarrow$ . The local Green's function is given by

$$G_{\tau\uparrow}^0 = \frac{q}{z} + \frac{1-q}{2} \left[ \frac{1}{z - \frac{1}{2}U_{\tau\uparrow} \cos 2\theta} + \frac{1}{z + \frac{1}{2}U_{\tau\uparrow} \cos 2\theta} \right], \quad (8)$$

where  $U_{\tau\uparrow} = A_{\text{eff}} + B = 2$  eV. The renormalized quasiparticle bandwidth is given by  $q = \frac{1}{4} \sin^2 2\theta$ . This width is equivalent to that obtained with slave-boson methods[11]. In addition, the method described here also provides information on the incoherent spectral weights described by the terms preceded by  $\frac{1}{2}(1-q)$ . For  $q$  close to unity, the spin-up  $\tau$  density of states is close to the independent-particle bandwidth. Note that, although  $q \rightarrow 1/4$  when  $\theta \rightarrow \pi/4$ , the Green's function gives the full bandwidth. When  $q$  decreases, a renormalized quasiparticle band  $q\varepsilon_{\mathbf{k}\tau\uparrow}$  is found between the upper and lower incoherent bands. This is the situation found for  $\text{CrO}_2$ , which is expected to be close to a metal-insulator transition[6], see Fig. 2(b). Upon further increasing the Coulomb term  $U_{\tau\uparrow}$ , the system goes through a Brinkman-Rice transition[12] and the quasiparticle peak disappears ( $q = \theta = 0$ ). In this limit, the model reduces to the Hubbard-I approximation[13]. The value for  $q$  can be found from minimization of the free energy as in Kotliar and Ruckenstein[11].

Despite the added difficulty of including the  $dd$  multiplet structure, an intuitive physical picture appears. In the ground state, all the orbitals, apart from the spin-up  $\tau_a$  states, are either full or empty. When adding an electron in a  $\tau_{a\uparrow}$  orbital, it can form a quasiparticle with the background of  $\tau_{a\uparrow}$  electrons. Therefore spin-up density of states is found at the Fermi level, see Fig. 3(b).

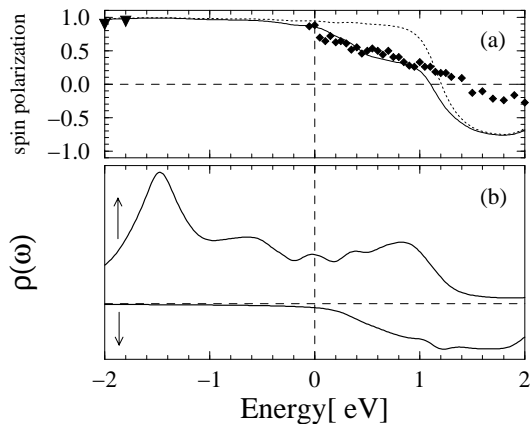


FIG. 3: (a) The spin polarization with (solid) and without (dotted) the inclusion of the  $S_z = 1/2$  component of the Fermi states.; (b) The density of states in the region of the Fermi level broadened with a Lorentzian with a width of 0.25 eV.

For addition of a  $\tau \downarrow$  electron, we can distinguish several situations. The local moment has two components:  $|d_{i,xy\uparrow}d_{i\tau_a\uparrow}\rangle$ , where  $a = 0, 1$ . Adding a  $\tau_{a'}$  electron to this state always results in a doublet state when  $a' = a$ , see the dotted line in Fig. 2(b). For  $a' \neq a$ , the chances of reaching a quartet and a doublet state are  $\frac{1}{3}$  and  $\frac{2}{3}$ , respectively; see the solid line in Fig. 2(b). It is important to note that, although the same quartet states  $|d_{xy\uparrow}d_{\tau_0\uparrow}d_{\tau_1\uparrow}\rangle$  ( ${}^4B_1$ ) are involved, the spin-up and spin-down  $\tau$  density of states are essentially different. Due to the on-site interactions, the spin-down  $\tau$  electron does not form a quasiparticle with the background of spin-up electrons and therefore feels the full Coulomb repulsion. Hence, only incoherent spectral weight is observed. In addition, the hopping of the spin-up  $\tau$  electron in the positive background is hindered by the ferromagnetic double-exchange mechanism[14, 15]. The reduction of the bandwidth by a factor of three is essential to prevent the spin-down band from crossing the Fermi level

(Obviously, this would lead to a contradiction with our assumption that the ground state is fully polarized). For all the other states, no quasiparticle states can be formed since the electrons feel the full Coulomb interaction for that particular multiplet. For example, the  $xy \uparrow$  electron-removal states are pushed to higher binding energies, see Fig. 2(c). The  $xy \downarrow$  electron-addition states are also pushed to higher energies above the Fermi level and split since two different doublet states can be formed with the background of  $|d_{i,xy\uparrow}d_{i\tau_a\uparrow}\rangle$  local moments.

The resulting spin polarization is shown in Fig. 3(a). For a better comparison with experiment a small Lorentzian broadening of 0.25 eV has been added. Below the Fermi level, a spin polarization close to 100% is found. Up to 0.1-0.2 eV above the Fermi level, the quasiparticle character dominates and the spin polarization is close to 100%. At higher energies above the Fermi level, the local moment character becomes important and the spin polarization decreases to approximately 50%. It then slowly decreases up to 1 eV, when it changes sign as a result of the spin-down  $e_g$  density of states. From the comparison with and without the inclusion of the  $S_z = 1/2$  component of the quartet state, it is obvious that restriction to a single Slater determinant leads to a poor description of the spin polarization close to the Fermi level, see Fig. 3(a).

In conclusion, we have demonstrated the importance of including the competition between quasiparticle and local-moment behavior in the description of the spin polarization of  $\text{CrO}_2$ . Although the discussion has been restricted to  $\text{CrO}_2$ , it is obvious that comparable behavior can be expected for other transition-metal compounds, such as the manganese perovskites showing colossal magneto resistance and even in much more delocalized systems such as Ni metal[16].

The contents of this paper were supported by the Laboratory for Nanoscience, Engineering, and Technology under a grant from the U.S. Department of Education. MvV is supported by the U.S. Department of Energy (DE-FG02-03ER460097).

- 
- [1] For a review see S. A. Wolff, D. D. Awschalom, R. A. Buhrmann, J. M. Daughton, S. von Molnár, M. L. Roukes, A. Y. Chtchelkanova, and D. M. Treger, *Science* **294**, 1488 (2001).
- [2] I. I. Mazin, *Phys. Rev. Lett.* **83**, 1427 (1999).
- [3] G. Schmidt, D. Ferrand, L. W. Molenkamp, A. T. Filip, and B. J. van Wees, *Phys. Rev. B* **62**, R4790 (2000).
- [4] K. Schwarz, *J. Phys. F* **16**, L211 (1986).
- [5] I. Mazin, D. J. Singh, and C. Ambrosch-Draxl, *Phys. Rev. B* **59**, 411 (1999).
- [6] M. Korotin, V. I. Anisimov, D. I. Khomskii and G. A. Sawatzky, *Phys. Rev. Lett.* **80**, 4305 (1998).
- [7] L. Craco, M. S. Laad, and E. Müller-Hartmann, *Phys. Rev. Lett.* **90**, 237203 (2003).
- [8] K. P. Kämper, W. Schmitt, G. Güntherodt, R. J. Gambino, and R. Ruf, *Phys. Rev. Lett.* **59**, 2788 (1987).
- [9] D. J. Huang *et al.*, *Phys. Rev. B* **67**, 214419 (2003).
- [10] J. S. Griffith, *The theory of transition-metal ions* (Cambridge University Press, Cambridge, 1961).
- [11] G. Kotliar and A. E. Ruckenstein, *Phys. Rev. Lett.* **57**, 1362 (1986).
- [12] W. F. Brinkman and T. M. Rice, *Phys. Rev. B* **2**, 4302 (1970).
- [13] J. Hubbard, *Proc. Roy. Soc. (London) A* **281**, 401 (1964).
- [14] C. Zener, *Phys. Rev.* **82**, 403 (1951).
- [15] P. W. Anderson and H. Hasegawa, *Phys. Rev.* **100**, 675 (1955).
- [16] B. Sinkovic, L. H. Tjeng, N. B. Brookes, J. B. Goedkoop, R. Hesper, E. Pellegrin, F. M. F. de Groot, S. Altieri, S. L. Hulbert, E. Shekel, and G. A. Sawatzky, *Phys. Rev. Lett.* **79**, 3510(1997).